

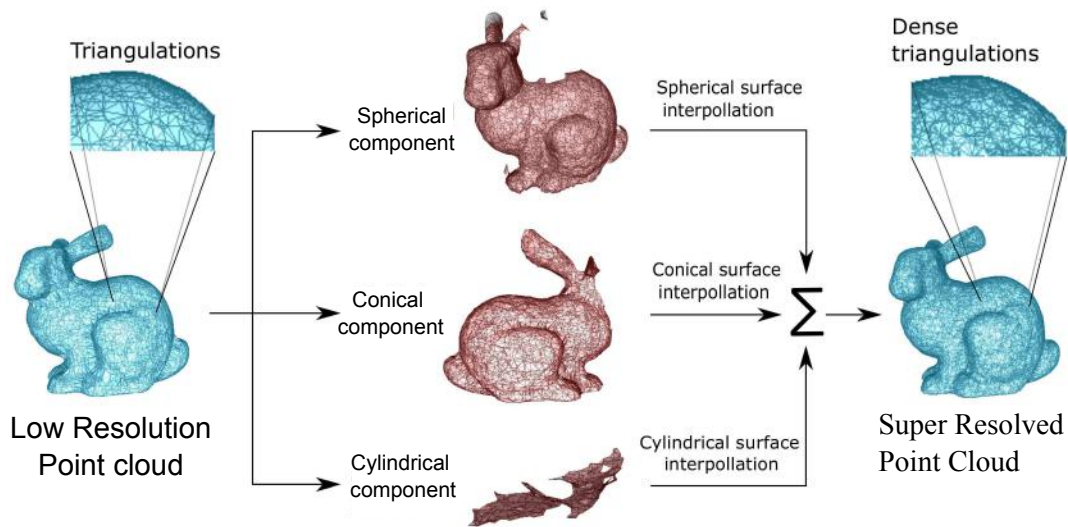
# 3D Object Super Resolution using Metric Tensor and Christoffel Symbols

Syed Altaf Ganihar<sup>\*</sup>  
B.V.Bhoomaraddi College of  
Engineering and Technology  
Hubli-India  
altafganihar@gmail.com

Shankar Setty  
B.V.Bhoomaraddi College of  
Engineering and Technology  
Hubli-India  
shankar@bvb.edu

Shreyas Joshi  
B.V.Bhoomaraddi College of  
Engineering and Technology  
Hubli-India  
shreyasvj25@gmail.com

Uma Mudenagudi  
B.V.Bhoomaraddi College of  
Engineering and Technology  
Hubli-India  
uma@bvb.edu



## ABSTRACT

In this paper we address the problem of 3D super resolution. 3D super resolution is a process of generating high resolution point cloud, given a low resolution point cloud. We model 3D object as a set of Riemannian manifolds in continuous and discretized space. We propose to use Riemannian metric tensor and Christoffel symbols as a set of features to capture the inherent geometry of the 3D object. We propose a learning framework to decompose 3D object using metric tensor and Christoffel symbols into a set of basis functions to selectively super resolve the 3D object. We demonstrate the proposed algorithm on 3D objects and achieve better results than reported in literature.

## Keywords

Super Resolution, Point cloud, Riemannian manifold, Metric tensor, Christoffel symbols, Differential geometry

<sup>\*</sup>Corresponding author

## 1. INTRODUCTION

In this paper we address the problem of 3D super resolution. Given a 3D low resolution point cloud data, super resolution technique aims to generate high resolution 3D point cloud data. The super resolved 3D point cloud data needs to preserve the geometric quality of the model and at the same time increase the resolution of the 3D object. 2D images are more stressed to visualize as compared to 3D models which provide additional information of geometrical and topological behavior of the object. However, super resolution of 3D models was little addressed as compared to 2D images. We first model the 3D object as a set of Riemannian manifolds in continuous space. We then use metric tensor and Christoffel symbols as geometric features to decompose the 3D object into a set of basis functions. Selective interpolation technique is adopted to super resolve the decomposed low resolution basis functions into high resolution 3D object. Title figure shows the detailed high resolution 3D object and the proposed process of generating super resolved object.

With the availability of devices such as laser range scanner, Microsoft Kinect [22], time-of-flight (ToF) cameras or flash LIDARS, acquiring 3D models from real world objects is quite common. However, generation of high resolution 3D models from low resolution models remains a complex and time consuming problem. Regardless of the scanning device used there is a limit on achieving high resolution 3D point cloud data and also acquisition of data is affected by noise, occlusion, illumination, deformation or limitation of capturing environment. Limitations can also be due to acquisition from a long distance and non-collaborated target object.

The problem of 3D super resolution arises in a number of applications which includes; (i) 3D models of animation movies (ii) digital preservation [25, 24] of cultural heritage sites, (iii) 3D model reconstruction - eg., detailing the statues, pillars, monuments, etc. (iv) transmission of 3D models via internet, where low resolution data transmitted needs to be detailed completely into high resolution models at the receiver, (v) zooming of particular region of interest and (vi) building of high quality 3D medical models, mechanical models, etc.

The 3D point cloud data acquired by 3D scanning devices, provide the geometric information of the sampling points on the surfaces of physical objects. The geometric properties in 3D point cloud data, such as ridges and corners which are composed of the geometric discontinuities, contain the important information of physical objects which often require special attention to achieve high accuracy and reliability. Therefore, feature extraction is essential to 3D point cloud data processing. Most of the 3D methods in literature use 3D shape features. Eg., 3D SURF descriptors [10], 3D Spatial Pyramids [13], Scale-dependent and scale-invariant local 3D shape descriptors [17], 3D SIFT [19] and volumetric feature SHD [20], local tensors [14], regional point descriptors extracted from range data [6]. However, we propose to use features extracted from the inherent geometry of 3D objects for super resolution. Metric tensor together with Christoffel symbols captures the unique set of geometric features that are inherent to the 3D object. The intuitive parameter for any 3D object is surface curvature. However surface curvature directly does not provide the inherent geometry of the 3D object[12]. To address this issue of 3D super resolution we propose a set of features based on metric tensor and Christoffel symbols. The geometric features, Riemannian metric tensor and Christoffel symbols could be used to address problems, which can be modeled as a manifold, like segmentation, reconstruction, registration, categorization and super resolution.

There have been several different approaches for super resolution to generate high resolution models. Eg., Joint Bilateral Upsampling (JBU) [11], spatial resolution and depth precision based iterative bilateral filtering [27], merging of probabilistic scan aligned depth images to obtain a single

depth [5], visual feedback based spatio-temporal filter [21], graph cut based space and time super resolution[16] and depth super resolution by rigid body self-similarity in 3D [8]. All these SR approaches can be broadly categorized into methods that (i) use a single image, (ii) merge information from multiple aligned viewpoint images (iii) call an external database of high-resolution exemplars or, (iv) use 3D point cloud data. We employ, 3D point cloud data as input to the proposed super resolution framework and super resolve to obtain a high resolution 3D object. Patra et al. [18] presents an approach of joining the 3D point cloud data obtained via Kinect with multiple images obtained from HD cameras to obtain high resolution dense point cloud. We propose to use a learning based approach to decompose the 3D object into a set of basis functions from the point cloud data. The learning based approach learns the Riemannian metric tensor and Christoffel symbols as features and decompose the 3D object into 3 basis functions viz. sphere, cone and cylinder.

Most of the super resolution algorithms involves selecting sample data from collection of depth patches, which are from within the input or external database. In [1] super resolved model is assembled by selecting from a collection of depth patches. Likewise [8] carries out SR by exemplars. In [16] selective super resolution involves selecting sample data. However, we propose selective SR technique to super resolve the decomposed basis functions obtained via Riemannian metric tensor and Christoffel symbols into 3D object.

We reiterate that 3D super resolution is less addressed problem than 2D super resolution and propose generation of super resolved 3D point cloud using geometrical features Riemannian metric tensor and Christoffel symbols using supervised learning approach. The basis functions for set of basic shapes are learned and are used in the super resolution process. In this paper we consider 3 basic shapes sphere, cone, cylinder and the given 3D object is decomposed into basic shapes, selective interpolation is adopted to super resolve the components. The selectively super resolved components are merged to generate the high resolution 3D object. Towards this we make the following contributions:

1. We model 3D object as a set of Riemannian manifolds in the continuous space and discretized space.
2. We propose to use Riemannian metric tensor and Christoffel symbols to address the problem of 3D super resolution.
3. We propose learning based approach to decompose the 3D object into a set of basis functions in order to selectively super resolve the components.
4. We demonstrate the proposed super resolution framework on different 3D objects and achieve better error rate than reported in the literature.

In Section 2 we explain our framework of 3D super resolution. In Section 3 we describe the geometric features. In Section 4 we discuss the learning based decomposition required for selective super resolution. In Section 5 we present the experimental results of the proposed method. We provide the conclusions in Section 6.

Permission to make digital or hard copies of all or part of this work for personal or classroom use is granted without fee provided that copies are not made or distributed for profit or commercial advantage and that copies bear this notice and the full citation on the first page. To copy otherwise, to republish, to post on servers or to redistribute to lists, requires prior specific permission and/or a fee.

ICVGIP '14, December 14 - 18 2014, Bangalore, India  
Copyright 2014 ACM 978-1-4503-3061-9/14/12 ...\$15.00.

## 2. 3D SUPER RESOLUTION

We model the given 3D object in a Euclidean space as a set of Riemannian manifolds. Let  $V(x, y, z)$  be a 3D object in the Euclidean space and is modeled as,

$$V(x, y, z) \mapsto \Psi(\mathcal{M}_i, g_i) \quad (1)$$

where  $i \in Z^+$  and  $i \leq n$  and  $\mathcal{M}_i, g_i$  represent the Riemannian manifolds.

Set of Riemannian manifolds constitutes a continuous space and 3D point cloud represented in a Euclidean space is a sampled version of this continuous space. To capture the inherent geometry in Riemannian space, we need to model the 3D object as a set of Riemannian manifold to account for the discontinuities in the geometry. A Riemannian manifold is a smooth construct which alone cannot represent the inherent geometry of the 3D object. This necessitates the need of piecewise smooth Riemannian manifold.

When we have a unique mapping of 3D Euclidean space to Riemannian space, the claim is there exists a unique mapping in the discretized (sampled) version of the 3D Euclidean space to Riemannian space. 3D point cloud in Euclidean space can be represented by a unique discretized set of Riemannian manifolds. Given a low resolution 3D point cloud, aim is to generate a high resolution 3D point cloud with magnification factor of  $r > 1 \in R^+$ . For any 3D point cloud there exists a unique map of set of Riemannian manifolds and this property is also true for samples with varied sampling rate since, mapping is unique in the continuous space.

Riemannian manifold or Riemannian space  $(\mathcal{M}, g)$  [12] is a real smooth differential manifold  $\mathcal{M}$  equipped with an inner product  $g_p$  on the tangent space at each point  $p$  and is given by,

$$p \mapsto g_p(X(p), Y(p)) \quad (2)$$

where the mapping from  $p \mapsto g_p$  is a smooth function with  $X(p)$  and  $Y(p)$  being vector fields in the tangent space of the 3D model at point  $p$ . The family  $g_p$  of inner products is called Riemannian metric tensor.

Typical super resolution methods involve several kinds of interpolation techniques to generate missing data. Here we try to capture the geometry of the 3D object using 'n' basis functions. These 'n' basis functions are used to interpolate components of low resolution points respectively along the 'n' basis functions.

In general the 3D objects exhibit geometrical similarities towards basic shapes like sphere, cone and cylinder. The geometrical similarities of the 3D object towards the basic shapes can be established by modeling the 3D object as a set of Riemannian manifolds  $\mathcal{M}_i$ ,

$$\Psi = \{(\mathcal{M}_i, g_i) | i \in \{1, 2, 3\}\} \quad (3)$$

with every  $i^{th}$  manifold being associated with a Riemannian metric  $g_i | i \in \{1, 2, 3\}$  for the three basic shapes sphere, cone and cylinder. The 3D objects hence comprise of superposition of basic geometrical properties on a local basis.

The geometric relation of the 3D object with basic shapes can be uniquely captured using Riemannian metric tensor and Christoffel symbols. The Riemannian metric tensor on the manifold  $\mathcal{M}$  is defined as a family of the inner products given by,

$$g_p : T_p\mathcal{M} \times T_p\mathcal{M} \mapsto R | \forall p \in \mathcal{M} \quad (4)$$

where  $T_p\mathcal{M}$  represents the tangent space at each point  $p$  on the manifold  $\mathcal{M}$ . The inner product  $g_p$  on the manifold  $\mathcal{M}$  defines a smooth function from  $\mathcal{M} \mapsto R$ . Given a Riemannian manifold  $(\mathcal{M}, g)$  there exists a unique affine connection  $\nabla$  on  $\mathcal{M}$  that is symmetric and compatible with  $g$  [12]. The uniqueness of the affine connection and the compatibility with the metric  $g$  is described in Theorem 1.

**THEOREM 1.** *A Riemannian manifold  $(\mathcal{M}, g)$  admits precisely one symmetric connection compatible with the metric. This particular connection is called the Riemannian connection or the Levi Civitta connection.*

The affine connection  $\nabla$  is called the Levi Civitta connection if

1. It preserves the metric i.e.,  $\nabla g = 0$
2. It is torsion free. i.e., for any vector fields  $X$  and  $Y$  we have,

$$\nabla_X Y - \nabla_Y X = [X, Y] \quad (5)$$

$[X, Y]$  is the Lie Bracket [12] of the vector fields  $X$  and  $Y$ .

The components of the Levi Civitta connection with respect to a system of local co-ordinates are called Christoffel symbols [12].

According to Theorem 1 a Riemannian manifold can be represented by the unique pair of Riemannian metric tensor and Christoffel symbols and equation 1 can be written as,

$$f : V(x, y, z) \mapsto \Phi(g_i, \Gamma_i) \quad (6)$$

where  $g_i$  and  $\Gamma_i$  represent the metric tensor and Christoffel symbols  $\forall i \in Z^+$ . The uniqueness and the compatibility of the metric tensor and Christoffel symbols is harnessed to establish a one to one mapping from the 3D object space  $\Phi$  to the metric tensor and Christoffel symbols space.

we reiterate that the 3D object exhibits geometrical similarities towards the basic geometrical shapes like sphere, cone and cylinder. Due to these similarities there exists a many to one mapping from the  $\Psi$  space (metric tensor and Christoffel symbols space for a given 3D object) to the metric tensor and Christoffel symbol space  $\Omega$  for the basic shapes and is given by,

$$\zeta : \Phi(g_i, \Gamma_i) \mapsto \Omega(g_j, \Gamma_j) \quad (7)$$

where  $g$  and  $\Gamma$  represent the metric tensor and Christoffel symbols with  $i \in Z^+$  and  $j \in \{1, 2, 3\}$ .

The components of the metric tensor and Christoffel symbols for the basic shapes can be regarded as the basis functions in a 3 dimensional space  $\Lambda$ . The mapping  $\zeta$  can be described as the resolution of the components of the metric tensor and Christoffel symbols in terms of the basis functions  $\xi_1, \xi_2, \xi_3$  for sphere, cone and cylinder respectively in  $\Lambda$ . Hence the given 3D object in the 3D point space  $R^3$  can be mapped to the basis functions  $\xi_1, \xi_2, \xi_3$  in  $\Lambda$ .

$$\chi : V(x, y, z) \mapsto \Lambda(\xi_1, \xi_2, \xi_3) \quad (8)$$

Equation 8 maps the 3D object in the Euclidean space to the component space  $\Lambda$  and is used to super resolve the 3D object along the three basis functions  $\xi_1, \xi_2, \xi_3$  using selective super resolution. In this process we use geometrical features Riemannian metric tensor and Christoffel symbols in a supervised learning approach to resolve the 3D object along the three basis functions.

### 3. FEATURES

The preliminary step for the proposed super resolution algorithm is the identification of the inherent geometry in the given 3D object. The identification of the inherent geometry is carried out with the help of a supervised learning approach, with Riemannian metric tensor and Christoffel symbols as geometric features. The given 3D object is modeled as a set of Riemannian manifolds  $(\mathcal{M}_i, g_i)$  to extract the geometric features metric tensor and Christoffel symbols.

#### 3.1 Metric Tensor

The metric tensor  $g_{\mu\nu}$  is a symmetric tensor and in 3-dimensions comprises of 6 independent components. The metric tensor gives the quantitative measure for the deviation in the manifold from the Euclidean space. The inner product or the arclength of a curve in the manifold as given by equation 4 can be computed with the help of the metric tensor and is given by,

$$ds^2 = \sum_{\mu=1}^3 \sum_{\nu=1}^3 g_{\mu\nu} dx^\mu dx^\nu \quad (9)$$

where  $ds^2$  is the arclength of an infinitesimal curve on the manifold and  $dx^\mu, dx^\nu$  are the contravariant tangent vectors in the tangent plane of the manifold.

The deviation in the arclength  $ds^2$  from the Euclidean distance function as shown in Figure 1, gives a measure of the metric tensor  $g$ . To compute the metric tensor we calculate the arclength  $ds^2$  as the geodesic distance between two neighboring points on a local patch as shown in Figure 1. We propose to use Algorithm 1 to compute the geodesic distance between a pair of points on the 3D point cloud.

**Data:** Pair of points  $v_1 v_2$  on the manifold to compute the geodesic distance.

**Result:** Geodesic distance between the pair of points.

initialization;

do dist  $\leftarrow$  0;

$k \leftarrow$  2;

$k1 \leftarrow$  2;

$i \leftarrow$  1;

$I_1 \leftarrow$  0;

**while**  $v_2 \notin I_1$  **do**

$I_1 \leftarrow$  k-nnsearch( $v_1, k$ );

$k \leftarrow k + 1$ ;

**end**

**while**  $v_1 \notin I_2$  **do**

$I_2 \leftarrow$  k-nnsearch( $v_2, k1$ );

$k1 \leftarrow k1 + 1$ ;

**end**

$I_3 \leftarrow I_1 \cap I_2$ ;

**while**  $i \neq \text{size}(I_3)$  **do**

    dist  $\leftarrow$  dist + EuclideanDistance( $I_3[i], I_3[i-1]$ );

$i \leftarrow i + 1$ ;

**end**

**Algorithm 1:** Geodesic distance computation on a pair of points on a point cloud.

In matrix notation the relation between the arclength  $ds$  and components of the metric tensor  $g$  is given by,

$$ds^2 = \begin{pmatrix} dx^1 & dx^2 & dx^3 \end{pmatrix} \begin{pmatrix} g_{11} & g_{12} & g_{13} \\ g_{21} & g_{22} & g_{23} \\ g_{31} & g_{32} & g_{33} \end{pmatrix} \begin{pmatrix} dx^1 \\ dx^2 \\ dx^3 \end{pmatrix} \quad (10)$$

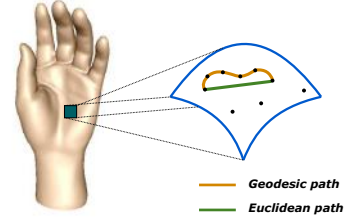


Figure 1: The metric computation for a 3D object is carried out on a local tangent plane by computing the deviation of the geodesic distance from the Euclidean distance.

The metric tensor consist of 6 independent components in 3-dimension. To compute the components of metric tensor a minimum of 6 pair of points are required for which the geodesic distances has to be computed. The geodesic distance is computed for 6 pair of points on the tangent plane of the manifold using Algorithm 1. Equation 10 is used to solve for the components of the metric tensor by using the 6 geodesic distances and the contravariant vectors  $dx_\mu$  and  $dx_\nu$  in the tangent plane.

#### 3.2 Christoffel Symbols

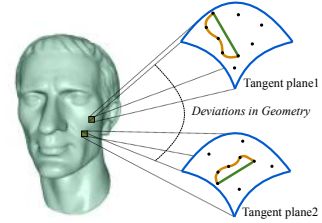


Figure 2: The computation of Christoffel symbols for a 3D object is carried out on a pair of neighboring local tangent planes by computing the deviations in the metric tensor over the tangent planes.

The Christoffel symbols give a measure of the deviation of the metric tensor as a function of position. The Christoffel symbols in 3-dimensions comprises of 18 independent components. The relation between metric tensor and Christoffel symbols is given by,

$$\Gamma_{\mu\nu}^\sigma = \frac{1}{2} \sum_{\rho=1}^3 g^{\sigma\rho} \left\{ \frac{\partial g_{\rho\mu}}{\partial x^\nu} + \frac{\partial g_{\rho\nu}}{\partial x^\mu} - \frac{\partial g_{\mu\nu}}{\partial x^\rho} \right\} \quad (11)$$

Equation 11 suggests that the computation of Christoffel symbols is dependent on the first derivative of metric tensor. The derivative operator in non-Euclidean space does not preserve the tensorial attributes of Christoffel symbols. They preserve the tensorial attributes under certain non-linear transformations. Equation 11 provides a pseudo-tensor which is utilized as one of the features in the proposed 3D object decomposition.

The Christoffel symbols are computed from the metric tensor values for every 12 pair of points belonging to two neighboring tangent planes on the manifold. The computation of the Christoffel symbols for a pair of neighboring tangent planes is as shown in Figure 4. The Christoffel symbols represent the deviations in the metric tensor from one tangent plane to another due to the phenomenon of parallel transport on a curvilinear surface [26, 15, 9, 12].

Riemannian metric tensor and Christoffel symbols together constitute a unique pair to represent a 3D object as given in Theorem 1. This property is utilized to decompose to decompose a given 3D object into 3 basic shapes for selective super resolution process.

#### 4. LEARNING AND DECOMPOSITION FOR SELECTIVE SUPER RESOLUTION

For a selective super resolution, there is a need to decompose a given 3D object into 3 basic shapes. The decomposition of 3D objects is carried out using a support vector machine framework [3]. The support vector machine is best suited for the decomposition problem as it maps the features for classification into multidimensional vector space and supports non-linear kernels for classification. The features used for the decomposition comprise of 24 independent components which are in turn dependent on the geometrical position of the point over which the features are computed. The normalization of the features is carried out by utilizing the positional dependence of the features for the 3D objects. The features for the training dataset are computed for unit scaled models to compensate for the scale dependence of the features. In our case we employ the  $3^{rd}$  order polynomial kernel for the learning framework in support vector machine as the features, metric tensor and Christoffel symbols exhibit positional dependence.

The decomposition of the 3D objects into basic shapes is carried out using a SVM framework and is depicted in Figure 3. The training data comprises of three classes of basic objects sphere, cone and cylinder which is fed to the SVM framework for learning. The features computed are fed to the SVM framework for decomposition of the 3D object into the basic geometrical shapes on a local patch comprising of 12 points. The classified patches are then segregated according to their respective classes to obtain the decomposed models which exhibit specific inherent geometry of either sphere, cone or cylinder.

The decomposition of objects into basic geometrical shapes assists us to process the 3D data in accordance with the inherent geometry of the 3D model. The input point cloud or 3D data is obtained either through a 3D scanning device like Microsoft Kinect or by running the sparse reconstruction algorithms like a Bundler [23] which computes the structure from motion. In either of the cases the obtained point cloud does not accurately portray the inherent properties of the scanned surface thereby warranting the need for super resolution algorithms which enhances the density of the point cloud. Most of the super resolution algorithms are based on interpolation techniques whose performance depends upon the geometrical properties of the scanned surface. Hence a single interpolation technique will not produce plausible results as the scanned surfaces will not have uniform geometrical properties throughout the surface. The proposed framework, relies on the geometrical decomposition of the

3D objects and hence the 3D model is super resolved based on the inherent geometry of the 3D object.

The decomposed components of a 3D object are super resolved in accordance with their inherent geometrical properties by using selective surface based interpolation techniques. Consider for example the spherically decomposed model is super resolved using spherical surface interpolation technique. Four points are required to fit a unique spherical surface over the given set of points. Hence the nearest neighbor search algorithm is invoked for every point in the spherically decomposed model to obtain the three nearest neighboring points. For every four set of points on the decomposed model, a spherical surface is determined to fit over the four set of points. The spherical surface is then used to carry out the interpolation for super resolving the point cloud. Similarly for cylindrical and conical models obtained after decomposition the interpolation is carried out on a local basis to obtain a selectively super resolved models. The selectively super resolved models are then fused to obtain the super resolved model which inherits similar geometrical properties compared to the original model.

#### 5. RESULTS AND DISCUSSION

The effectiveness of the proposed super resolution framework is demonstrated on models obtained from Stanford 3D scanning repository, AIM@SHAPE and . The algorithm is implemented on Intel(R) Core(TM) i7-4700MQ processor @ 2.40GHz and 8GB RAM with NVIDIA GeForce GT 755M graphics.

We demonstrate the proposed decomposition framework on models obtained from AIM@SHAPE dataset as shown in Figure 5. The training data includes unit sphere, unit cone and unit cylinder with an average of 40,000 points. The training feature vector contains 24 features 6 for metric tensor and 18 for Christoffel symbols computed for 40,000 points. The 3D object under consideration is fed to the SVM for decomposition of the 3D object into the basic geometrical shapes. The 3D object is divided into local patches comprising of 12 points each, which are fed to the SVM for classification into the basic models. The patches belonging to a particular class of basic model are extracted from the original object and are shown in Figure 5 for teapot, vase, hand and animal model.

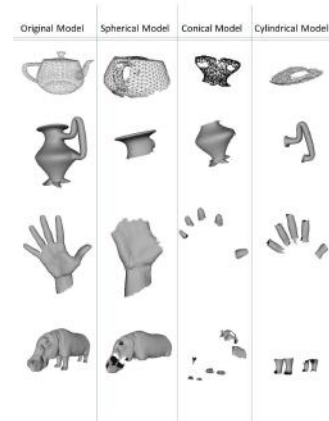


Figure 5: The decomposition of 3D objects into basic shapes like sphere, cone and cylinder.

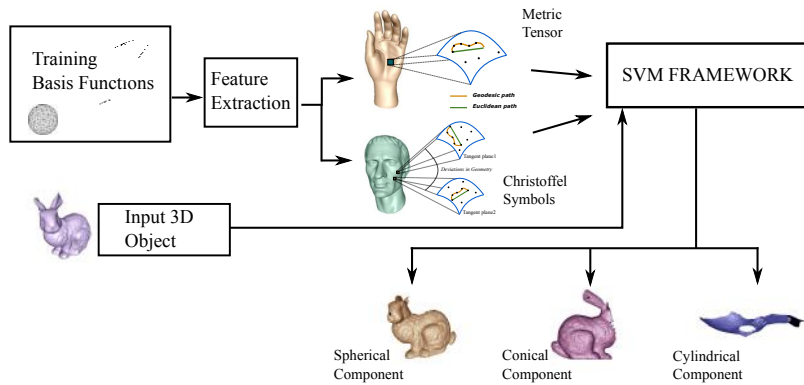


Figure 3: Decomposition of a given 3D object into basic shapes.

We demonstrate the results of the proposed super resolution framework using Stanford bunny point cloud subsampled by a factor of 2, 4 and 8 as shown in Figure 4. The bunny point cloud is subsampled by a factor of 2, 4 and 8 by using the mesh element sampling technique [4] and then subsequently super resolved using the proposed algorithm with a magnification factors of 2, 4 and 8. The figure shows the comparison of the decomposed models at different subsampled rates with the ground truth. The selectively super resolved model with magnification factors 2, 4 and 8 are compared with the ground truth model as shown in Figure 4. The selectively super resolved models are then merged to obtain the final super resolved model which is compared with the original ground truth. A similar approach is adopted for quadratic spline interpolation, cubic spline interpolation, Moving Least Square upsampling (MLS) and decision framework [7] super resolution techniques. The RMS error of the super resolved point cloud with magnification factors 2, 4 and 8 is 4.49%, 7.20% and 10.27% respectively with respect to the ground truth as shown in Figures 6 and 7.

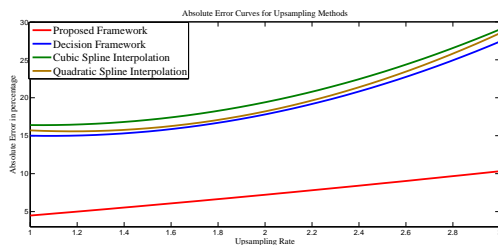


Figure 6: The plot of RMS error for the magnification factors 2, 4 and 8 for the proposed framework, [7], quadratic spline and cubic spline

The proposed super resolution algorithm is demonstrated on 3D objects acquired from Microsoft Kinect sensor for models with points 9324, 11514 and 10601 as shown in Figure 8. The super resolution is carried out with a magnification rate  $\approx 2$ . Surface reconstruction of the original and the super resolved 3D point clouds is carried out using the ball pivoting surface reconstruction algorithm with ball radius of 22.3692 world unit or 3% in absolute measure [2]. Figure 8 shows a betterment in the performance of the surface reconstruction algorithm for the super resolved model compared to the low resolution model.

Super Resolution Methods	RMS Error(in %)		
	Resolution Factor		
	2	4	8
MLS	67.18%	149.51%	225.36%
Cubic Spline Interpolation	15.51%	17.84%	27.33%
Quadratic Spline Interpolation	15.99%	19.03%	28.69%
Decision Framework [7]	15.59%	18.11%	28.43%
<b>Proposed Framework</b>	<b>4.49%</b>	<b>7.2%</b>	<b>10.27%</b>

Figure 7: The RMS error for the magnification factors 2, 4 and 8 for the proposed framework, Decision framework [7], quadratic spline and cubic spline.

## 6. CONCLUSION

We have addressed the problem of 3D super resolution. 3D super resolution is a process of generating high resolution point cloud, given a low resolution point cloud. We have modeled the 3D object as a set of Riemannian manifolds in continuous and discretized space. We use Riemannian metric tensor and Christoffel symbols as a set of features to capture the inherent geometry of the 3D object. We have proposed a learning framework to decompose 3D object using metric tensor and Christoffel symbols into a set of basis functions to selectively super resolve the 3D object. We have demonstrated the proposed algorithm on 3D objects and achieve better results than reported in literature.

## 7. REFERENCES

- [1] O. M. Aodha, N. D. F. Campbell, A. Nair, and G. J. Brostow. Patch based synthesis for single depth image super-resolution. In *Proceedings of the 12th ECCV - Volume Part III*. Springer-Verlag, 2012.
- [2] F. Bernardini, J. Mittleman, H. Rushmeier, C. Silva, and G. Taubin. The ball-pivoting algorithm for surface reconstruction. *IEEE Transactions on Visualization and Computer Graphics*, 5(4):349–359, Oct. 1999.
- [3] C. J. Burges. A tutorial on support vector machines for pattern recognition. *Data Mining and Knowledge Discovery*, 2:121–167, 1998.
- [4] M. Corsini, P. Cignoni, and R. Scopigno. Efficient and flexible sampling with blue noise properties of

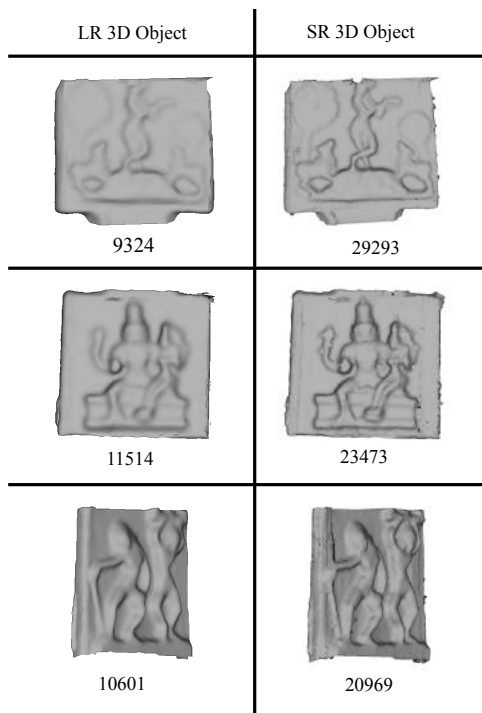


Figure 8: The super resolution of 3D point clouds using the proposed framework for models obtained using Microsoft kinect.

triangular meshes. *IEEE Transactions on Visualization and Computer Graphics*, 18(6):914–924, June 2012.

- [5] Y. Cui, S. Schuon, S. Thrun, D. Stricker, and C. Theobalt. Algorithms for 3d shape scanning with a depth camera. *Pattern Analysis and Machine Intelligence, IEEE Transactions on*, 35(5):1039–1050, May 2013.
- [6] A. Frome, D. Huber, R. Kolluri, T. BÅijlow, and J. Malik. Recognizing objects in range data using regional point descriptors. In *ECCV*, 2004.
- [7] S. A. Ganihar, S. Joshi, N. Patil, U. Mudenagudi, and M. Okade. Voting-based decision framework for optimum selection of interpolation technique for 3d rendering applications. In *Students’ Technology Symposium (TechSym), 2014 IEEE*, pages 270–275, Feb 2014.
- [8] M. Hornacek, C. Rhemann, M. Gelautz, and C. Rother. Depth super resolution by rigid body self-similarity in 3d. In *CVPR*. IEEE, 2013.
- [9] J. Jost. *Riemannian Geometry and Geometric Analysis*. Springer Universitat texts. Springer, 2005.
- [10] J. Knopp, M. Prasad, G. Willems, R. Timofte, and L. Van Gool. Hough transform and 3d surf for robust three dimensional classification. In *Proceedings of the 11th ECCV: Part VI*. Springer-Verlag, 2010.
- [11] J. Kopf, M. F. Cohen, D. Lischinski, and M. Uyttendaele. Joint bilateral upsampling. In *ACM SIGGRAPH*, 2007.
- [12] S. Kumaresan. *A course in differential geometry and Lie groups*. Texts and readings in mathematics. Hindustan Book Agency, 2002.
- [13] R. J. Lopez-Sastre, A. Garcia-Fuertes, C. Redondo-Cabrera, F. J. Acevedo-Rodriguez, and S. Maldonado-Bascon. Evaluating 3d spatial pyramids for classifying 3d shapes. *Computers and Graphics*, 37(5):473–483, 2013.
- [14] A. S. Mian, M. Bennamoun, and R. Owens. Three-dimensional model-based object recognition and segmentation in cluttered scenes. *IEEE Trans. Pattern Anal. Mach. Intell.*, 28(10):1584–1601, Oct. 2006.
- [15] C. Misner, K. Thorne, and J. Wheeler. *Gravitation*. W.H. Freeman and Company, 1973.
- [16] U. Mudenagudi, S. Banerjee, and P. Kalra. Space-time super-resolution using graph-cut optimization. *Pattern Analysis and Machine Intelligence, IEEE Transactions on*, 33(5):995–1008, May 2011.
- [17] J. Novatnack and K. Nishino. Scale-dependent/invariant local 3d shape descriptors for fully automatic registration of multiple sets of range images. In *Proceedings of the 10th ECCV: Part III*. Springer-Verlag, 2008.
- [18] S. Patra, B. Bhowmick, S. Banerjee, and P. Kalra. High resolution point cloud generation from kinect and hd cameras using graph cut. In *VISAPP (2)’12*, 2012.
- [19] P. Scovanner, S. Ali, and M. Shah. A 3-dimensional sift descriptor and its application to action recognition. In *Proceedings of the 15th International Conference on Multimedia*. ACM, 2007.
- [20] P. Shilane and T. Funkhouser. Distinctive regions of 3d surfaces. *ACM Trans. Graph.*, 26(2), June 2007.
- [21] J. W. Silva, L. Gomes, K. Apaza-AgÅijero, O. R. P. Bellon, and L. Silva. Real-time acquisition and super-resolution techniques on 3d reconstruction. In *ICIP*, 2013.
- [22] J. Smisek, M. Jancosek, and T. Pajdla. 3d with kinect. In *Computer Vision Workshops (ICCV Workshops), IEEE International Conference on*, 2011.
- [23] N. Snavely, S. M. Seitz, and R. Szeliski. Photo tourism: Exploring photo collections in 3d. *ACM Trans. Graph.*, 25(3):835–846, July 2006.
- [24] B. Trinchão Andrade, O. R. Bellon, L. Silva, and A. Vrubel. Digital preservation of brazilian indigenous artworks: Generating high quality textures for 3D models. *Journal of Cultural Heritage*, June 2011.
- [25] A. Vrubel, O. R. P. Bellon, and L. Silva. A 3d reconstruction pipeline for digital preservation. In *CVPR*. IEEE, 2009.
- [26] S. Weinberg. *Gravitation and Cosmology: Principles and Applications of the General Theory of Relativity*. Wiley, New York, NY, 1972.
- [27] Q. Yang, R. Yang, J. Davis, and D. Nister. Spatial-depth super resolution for range images. In *Computer Vision and Pattern Recognition, 2007. CVPR ’07. IEEE Conference on*, 2007.

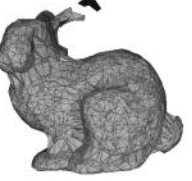
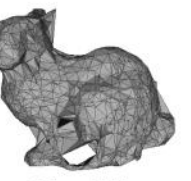
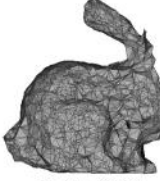
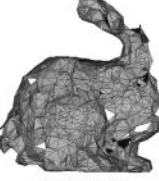
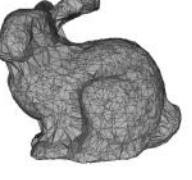
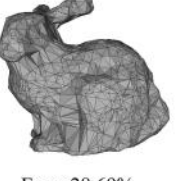
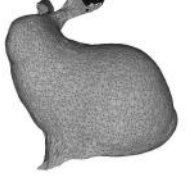
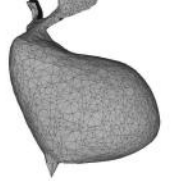
	SR 3D object			
	Resolution Factor $\approx 2$	Resolution Factor $\approx 4$	Resolution Factor $\approx 8$	
Spherical Component	 Points:8591	 Points:10895	 Points:9409	
Cylindrical Component	 Points:744	 Points:754	 Points:479	
Conical Component	 Points:7607	 Points:9490	 Points:8421	
<b>Ground Truth</b>	 14106	 Points:16936 Error:4.49%	 Points:21139 Error:7.2%	 Points:18309 Error:10.27%
<b>Cubic Spline Interpolation</b>	 Error:15.51%	 Error:17.84%	 Error:27.33%	
<b>Quadratic Spline Interpolation</b>	 Error:15.99%	 Error:19.03%	 Error:28.69%	
<b>Decision Framework [7]</b>	 Error:15.59%	 Error:18.11%	 Error:28.43%	
<b>MLS</b>	 Error:67.18%	 Error:149.51%	 Error:225.36%	

Figure 4: The super resolution of Stanford bunny point cloud subsampled by a factor of 2, 4 and 8 using the proposed framework, Cubic spline interpolation, Quadratic spline interpolation, Decision framework [7] and MLS.